Proceedings of 20th International Congress on Acoustics, ICA 2010

23-27 August 2010, Sydney, Australia

Noise reduction of an acoustical enclosure --- Mechanisms and prediction accuracy

Ye Lei (1, 2), Jie Pan (1) and Meiping Sheng (2)

(1) School of Mechanical Engineering, University of Western Australia, Nedlands WA 6009, Australia
(2) College of Marine, Northwestern Polytechnical University, Xi'an 710072, China

PACS: 43.40.AT, 43.55.KA

ABSTRACT

Noise reduction (NR) of an acoustical enclosure with flexible boundary walls has been predicted using the Statistical Energy Analysis (SEA) method by several authors. Although it is useful for a rough NR estimation, a large discrepancy often exists between the predicted and measured NR levels. Moreover, some physical mechanisms which may affect NR prediction were not addressed in the existing SEA models. The sources of the discrepancy were identified by investigating the limitation of SEA for system energy transfer in the entire frequency range of noise transmission, and the effect of enclosure wall coupling and sound-structural coupling on the NR and its prediction accuracy. This paper presents a modified SEA model, which includes the non-resonant response and more accurate transmission coefficient of finite panels, and compares the model prediction with experimental results. A reasonable agreement between the prediction and experiment was observed.

INTRODUCTION

An acoustical enclosure with enveloping panels is a vibro-acoustic system which may effectively reduce noise generated from running machines. Acoustical enclosure was a topic of research more than half a century ago. Lyon's work [1] on noise reduction of a rectangular enclosure had shown some physical insight of the noise transmission into the enclosure. In recent years, Ming and Pan [2] and several other researchers [3, 4] investigated NR of more complicated enclosures with coupled side-walls and partially opened cavities.

Prediction of NR of an acoustical enclosure is often required at the design and assessment stages of noise control. Although investigated by many authors, a large discrepancy often exists between the predicted and measured NR levels at low and middle frequencies. The non-resonant response of panels is an important physical mechanism causing such discrepancy. This phenomenon was proposed in Lyon's work [1], however, it is neglected in his analytical model. Crocker and Price [5] considered the non-resonant transmission into their research by using the mass law which bases on infinite plate theory. Sewell [6], Reynold [7] investigated the property of sound transmission of finite panels including bending stiffness effect and the prediction is more accurate than the classical mass law, but often overestimates the transmission loss because only the forced vibration is considered. Ming and Pan [2] considered the non-resonant transmission from the inner sound field to the outside one when predicting NR, but they added the sound power generated by non-resonant response to the sound power by resonant vibration in the total power calculation, and neglected the effect of structural-structural coupling on the sound-structural coupling and the power transferred back to the structure from the outside sound field. Renji et al. [8] analyzed the non-resonant response by treating it as a separate subsystem during SEA modelling at high frequencies. In their model, the sound transmission coefficient was calculated from Reynolds's formula [7], which set the forced radiation efficiency of finite panels to the inverse of the cosine of the angle of incidence. Davy [9] improved Cremer's theory by replacing the forced radiation efficiency of an infinite plate with that of a finite size panel and propoed a new approach to analyze the correction term of the bending stiffness in the frequency range where both structure and sound field have resonant modes.

In this paper, we focus on the accurate modelling of NR in the entire frequency range and the essential physical mechanisms that control the accuracy of NR. In the impoved SEA model, non-resonant response of every flexible panel is considered as a subsystem. Accuract expression of the sound transmission coefficient of finite panels is also adopted. Experiment has been carried out to verify the predicted results.

In the experiment, the radiated power from the enclosure is measured by both sound pressure method (SPM) and sound intensity method (SIM). Further more, as different definitions of NR [1, 5] exist, the level difference between the sound power level into the box and that into the laboratory room is employed in this study in order to minimize the prediction error coming from the reverberant time measurement.

EXPERIMENTAL STUDIES

Description of the experiment

The experimental work was conducted in a large laboratary room, whose volume is about 198m^3, with several furnitures and sound scattering items. The dimension of the acoustical

enclosure box is 0.868m×1.15m×1m. The aluminum box is made of one clamped and five simple-supported flexible panels. The panels have uniform thickness of 2.5mm. The Young's modulus, Poisson ratio and mass density of the panels are respectively 6.85×10^{10}Pa, 0.34, and 2700kg/m^3. The lid of the box is clamped by two steel frames with a flange between them. A small hole in one side panel is used to insert a pipe which connects a horn driver (No.1 loudspeaker) to generate high frequency noise in the box. In order to generate adequate low frequency noise, a loudspeaker (No.2 loudspeaker) backed by a loudspeaker box is placed at one inner corner of the enclosure. The measurements of low frequency and high frequency responses were taken separately. The schematic configuration of the enclosure is shown in Figure 1 and the measurement system is described in Figure 2.

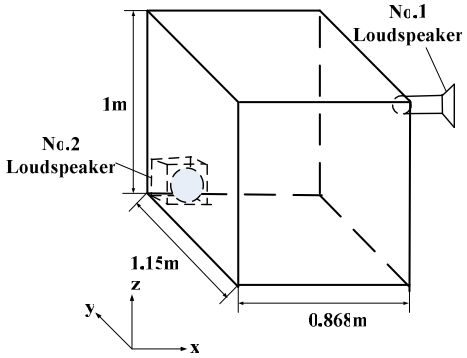

Figure 1. The acoustical enclosure box.

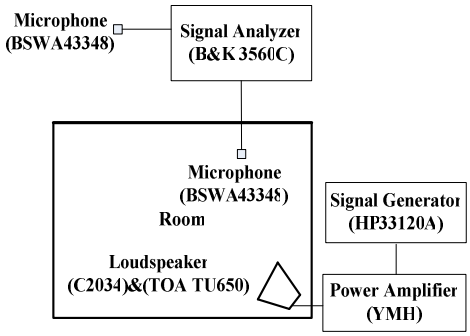

Figure 2. The measurement system.

Experimental results

The dissipation loss factor of the lid can be measured using the vibration decay method. In this study, the enclosure box is identical to that used by Ming and Pan [2], so the dissipation loss factor can be calculated from their empirical formula taking into account of the radiation loss and the edge loss [9]. The free radiation efficiency of finite panels is derivated from the approximating radiation ratio by Lei et al. [10], based on the analytical results for baffled plates by Xie et al. [11]. The forced radiation efficiency of finite panels is calculated by using Davy's expression [9] above the first non-Helmholtz natural frequency of the cavity and equals unity under this frequency. The simulation of these two kinds radiation efficiency is shown in Figure 3 and the corresponding dissipation loss factor of the lid panel is plotted in Figure 4. It can be found from the curves in Figure 4 that the forced radiation loss is greater than the structural loss, and the edge loss is not important to the total structural loss factor.

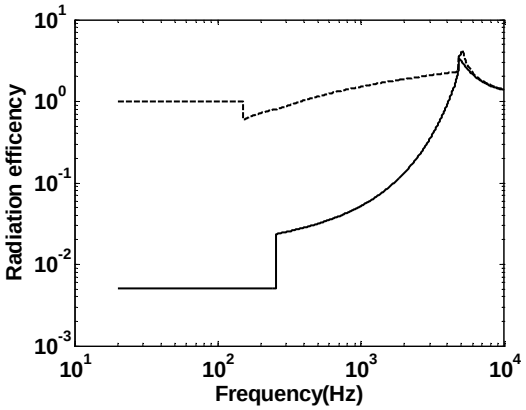

Figure 3. Radiation efficiency of the lid panel. (——: free radiation efficiency; -----: forced radiation efficiency)

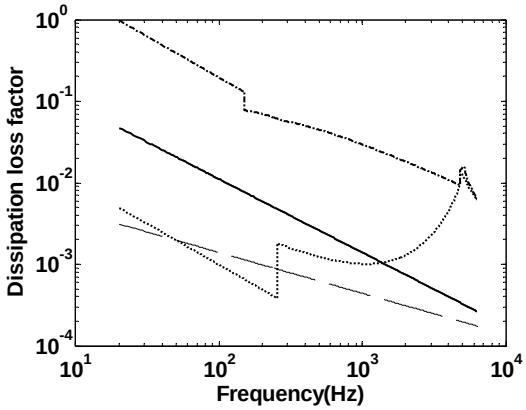

Figure 4. Dissipation loss factor of the lid panel. (——: predicted structural loss factor by Ming and Pan's empirical formula; ·····: predicted free radiation loss factor; -.-: predicted forced radiation loss factor; -----: predicted edge loss factor)

The dissipation loss factors of the internal sound field and external sound field are calculated by measuring their reverberation time T_{60},

$$\eta_a = \frac{2.2}{fT_{60}}, \tag{1}$$

where f is the central frequency in one-third Octave band, η_a is the dissipation loss factor of enclosed acoustic field. The results are plotted in Figure 5. Since there is no measured data at low frequencies, the curve fitting results for external sound field and Ming and Pan's results for internal sound field are also presented in the figure.

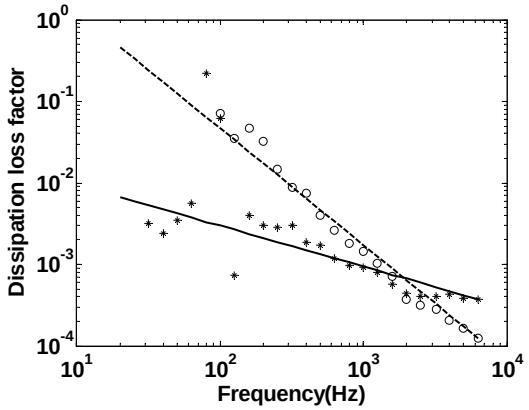

Figure 5. Dissipation loss factors of the sound fields. (——: calculated by Ming and Pan's formula;- * -: measured in the box; ------: fitted by this paper; -○-: measured in the room)

The arrangement of the response measurements by using different loudspeakers and testing methods are summarized in Tables 1 and 2, for acoustic field in the box and in the room respectively. The same case noted in both tables means that the experiments were carried out in the same time. The final physical quantities for calculation and comparison are sound pressure level and sound power level for the internal and external sound field, respectively. According to Tables 1 and 2, the experimental results are shown in Figures 6 and 7. The inner sound pressure levels, just measured by SPM, are also presented here in order to emphasize the source of the difference between the radiated sound power levels, in how much percent coming from the difference of the sources. By comparing the measured sound power levels using different measuring methods, it can be found that the discrepancy is smaller than 0.5dB above 400Hz for No.1 loudspeaker, and the discrepancy is negligible in the frequency range from 100Hz to 600Hz for No.2 loudspeaker. Thus, the input data for calculation are gained from two loudspeakers. From 400Hz to 6.3kHz, the data of No.1 loudspeaker is used, and when frequency below 400Hz, the data of No.2 loudspeaker is used. Therefore, the measurements are reliable in the entire frequency range of interest.

Table 1. The arrangement of measuring response in the box by using different loudspeakers

	Loudspeaker	*Measuring method*
Case 1	*No.2*	*SPM*
Case 2		
Case 3	*No.1*	*SPM*
Case 4		

Table 2. The arrangement of measuring response in the room by using different loudspeakers and measuring methods

	Loudspeaker	*Measuring method*
Case 1	*No.2*	*SPM*
Case 2	*No.2*	*SIM*
Case 3	*No.1*	*SPM*
Case 4	*No.1*	*SIM*

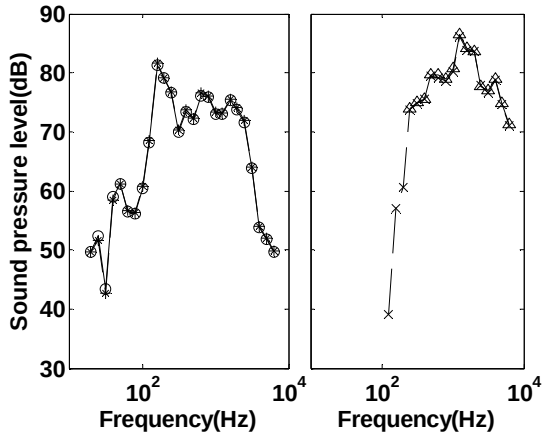

Figure 6. Sound pressure level in the box (Reference sound pressure: $2\times10^{-5}Pa$). (— * —: case 1;—○—: case 2;—△—: case 3;—×—: case 4)

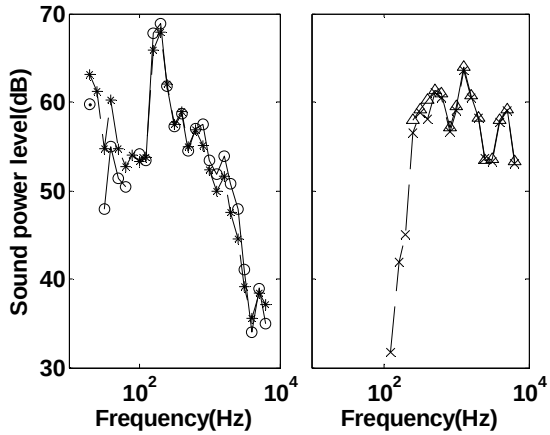

Figure 7. Sound power level in the room (Reference sound power: $1\times10^{-12}W$). (— * —: case 1;—○—: case 2;—△—: case 3;—×—: case 4)

THEORETICAL MODEL

Statistical energy analysis is a practical method for analyzing the power and energy in coupled vibro-acoustic systems. Classical SEA method is entirely based on the statistical theory and the energy conservation law, leading to averaged quantities obtained. Nevertheless it has been used in many practical applications, such as in noise control of aircraft structures. A full and accurate history of SEA is available in numerous references [12, 13]. In this section, we focus on analyzing NR using SEA.

The quantity of noise reduction is defined by following expression

$$NR = 10\log_{10}(W_s / W_r), \tag{2}$$

where W_s and W_r are respectively source power into the box and radiated power into the laboratory room.

Assuming the inner sound field is reverberant and the specific acoustic impedance equals 400kg/m^{2}s, if the measured quantity is sound pressure p, the relationship between the sound power into the field and sound pressure is described as follows

$$W_s = 10^{-4}\, p^2 V / T_{60}, \tag{3}$$

where V and T_{60} are the volume and the reverberant time of the sound field, respectively.

The sound power in the room is the sum of radiated power from all the structural subsystems, and given by

$$W_r = \sum_i \rho_0 c_0 S_i \sigma_i (E_i / m_i) , \quad (4)$$

where ρ_0 is the mass density of the air; c_0 is the sound speed in the air; σ_i ,S_i and m_i are the radiation efficiency, surface area and total mass of subsystem i, respectively; E_i is the averaged model energy of subsystem i.

In this paper, three frequency ranges are considered. At the lower frequencies, both the structure and the sound field are stiffness controlled.

In the intermediate frequency range, the air in the box behaves like a spring, while the panels of the wall structure have resonant response. In this frequency range, the air volume of the box allows the source power to be transmitted into the structure of the box in two paths. In the first path, the noise source dissipates energy in the box volume and transmits energy to the panels and excites them to behave in resonant way, and power input into each panel can be calculated by using the input surface mobility [14] of the finite panels,

$$W_i = \frac{1}{2} | p_a |^2 \ \mathrm{Re}\{M^s\} , \quad (5)$$

where p_a is the amplitude of the pressure of the sound field within the box, M^s is the input surface mobility of panel i.

The flexible panels of the box structure are treated as subsystems in the SEA model and their resonant vibration response could be obtained by solving the power flow balance equations. The power flow relationship between the resonant responses of panels is written as

$$\omega \eta_i E_i - \omega \sum_{j \neq i}^{I} \eta_{j,i} E_j = W_i , \quad (6)$$

where E_i is the resonant average modal energy of panel i, $\eta_{j,i}$ is the coupling loss factor between panel j and i, I is the total number of panels.

In the second path, sound energy inside the enclosure can be transferred by the non-resonant transmission way and hence the inner sound field should be modeled as a subsystem in this stage. The power flow balance equations between the non-resonant response and sound field are expressed as

$$\omega \eta_i E_{ii} - \omega \eta_{s,ii} E_s = 0 , \quad (7)$$

$$\omega \eta_s E_s - \omega \eta_{ii,s} E_{ii} = W_0 \quad . \quad (8)$$

where E_{ii} is the non-resonant average modal energy, E_s is the average energy of the source sound field, $\eta_{s,ii}$ is the coupling loss factor between the inner sound field and the non-resonant response of panel i, $\eta_{ii,s}$ is the reverse one, W_0 is the sound power in the box induced the non-resonant response. The detailed calculation formula of coupling loss factor in Eq.(7) and Eq.(8) is studied in work [8]. The modified transmission coefficient which used for calculating the sound-structural coupling loss factor is discussed in Davy's research [9] and the radiation efficiencies of the free and forced vibration are computed as proposed in the section of Experimental studies.

At the high frequencies, both the sound in the box and vibration in the flexible panels are modelled as diffuse fields. In this frequency range, the inner sound field couples with resonant response of panels in the SEA model, and this is the only difference from the first energy transmission path at the intermediate frequencies. The non-resonant response should also be considered in this frequency range. The power flow balance equations are described as

$$\omega \eta_j E_j - \omega \sum_{i \neq j, i=1}^{2I+1} \eta_{i,j} E_i = 0 , \quad (9)$$

$$\omega \eta_s E_s - \omega \sum_{j=1}^{2I} \eta_{j,s} E_j = W_0 . \quad (10)$$

Eqs.(9) and (10) reveal the power flow relationship between the air enclosure and other subsystems, including resonant and non-resonant response of panels. By solving Eqs.(9) and (10), average modal energy of each subsystem could be obtained. Finally, the total sound power in the room is calculated by putting the average modal energy of each structural subsystem into Eq.(4).

RESULTS AND DISCUSSION

As the enclosure box is excited by the internal sound field, the vibration energy of the wall panels of the box can be divided into two groups [15]. The first group is the "free" bending response, which only exists in finite structure and panel boundary reflection generates interaction of the bending waves with wavelength rather than that of the excitation sound wave. This type of panel response behaves in forms of resonant modes. In the second group, when the trace wavelength of the incident acoustic wave matches the panel bending wavelength, the forced vibration occurs. In this process, a lot of energy is transferred to the adjoining sound field because of large radiation efficiency. Accordingly, sound transmission not only comes from the "free" vibration, but also from the forced vibration, which are named resonant transmission and non-resonant transmission respectively.

Above the critical frequency of the panel, the sound transmission through the panels is dominated by resonant response mostly. Below the critical frequency, the sound transmission is controlled by both resonant and non-resonant response. The main reason of this physical mechanism at this frequency range is that the radiation efficiency of non-resonant response equals unity, whereas the resonant one is much smaller than unity, although the vibration level of resonant response has no great difference from the non-resonant part.

Figure 8 compares the sound power levels radiated from the enclosure box with and without including the non-resonant response into SEA model. The prediction results from Renji et al. [8] and Ming and Pan [2] are also plotted in the figure for comparison.

The model including both resonant and non-resonant transmission agrees well with the experimental result above 63Hz. The errors are smaller than 2dB except at low frequencies and above the critical frequency. There are two reasons for large errors at low frequencies: (1) The second loudspeaker provides deficient power to the system; (2) the basic hypotheses of SEA are not valid at these frequencies. The reason for the error above the critical frequency is the overestimated forced radiation efficiency.

The model including only resonant transmission produced a large difference, reaching 25dB, from the experimental result at some frequencies. This amount of discrepancy has also been obtained by Renji [8]. The comparison means that the non-resonant response plays significant role in transferring energy from the source field to the receiving room, especially at intermediate frequencies.

As mentioned above, the difference of calculation of transmission coefficient will cause considerable error. The higher value of NR predicted by Renji's theoretical model above the fundamental frequency of the inner sound field indicates that the outside power prediction is underestimated. This is because the forced transmission coefficient mentioned in their work was calculated from Reynolds's algorithm which improves the prediction accuracy relative to the classical mass law by including bending stiffness. However, the approximation of applying the infinite plate theory to the forced radiation efficiency causes the transmission loss inaccuracy in the frequency range between the fundamental frequency of the cavity and the critical frequency of the panel.

Although the predicted result by the model developed by Ming and Pan is more accurate than the prediction without including the non-resonant response in this study, it is still less accurate than that by the model including non-resonant response into the whole energy transfer route in this study. The non-resonant transmitted power, in Ming and Pan's research, is simply added to the total radiated sound power algebraically, ignoring the effect of other structural-structural and sound-structural coupling on the non-resonant response. Meanwhile, their model also neglected the power transferred back to the structure from the outside sound field, which is important when coupling between structure and the heavy medium is involved. Therefore, the non-resonant response should be included in the entire SEA energy transfer model and analyzed along with other subsystems. In addition, the forced transmission coefficient used in Ming and Pan's model is based on the classical mass law, which is for the infinite plate with negligible bending stiffness.

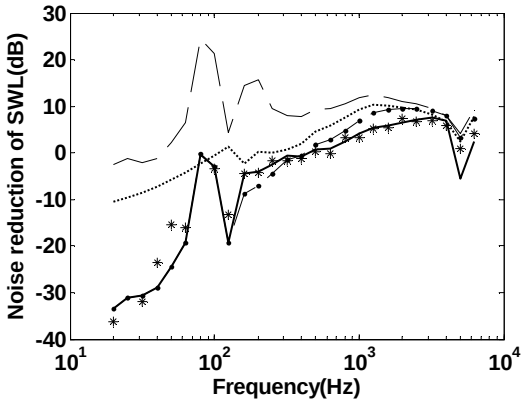

Figure 8. Difference of sound power level (ref: $1\times10^{-12}W$). (——: prediction by this study considering non-resonant response;–·–: prediction by this study ignoring non-resonant response; ……: prediction by Ming et al.'s model [2]; — —: prediction by Renji et al.'s model [8]; * : experimental results)

In order to explain the use of sound power to express the noise reduction, the differences of sound pressure level and sound energy level between the inner sound field and the outside reverberant room are also predicted in Figure 9 and Figure 10. The prediction is not as accurate as Figure 8, because the reverberant time and effective volume of the outside room should be used to compute the sound pressure level (SPL) and sound energy level (SEL). Therefore, the error from testing the reverberant time and the effective volume of the external room will enlarge the error of NR prediction and decrease the precision. In reality, the outside room is reverberated insufficiently, so the reverberant time used for calculating SPL and SEL at intermediate frequencies is obtained by the fitting method, as shown in Figure 5.

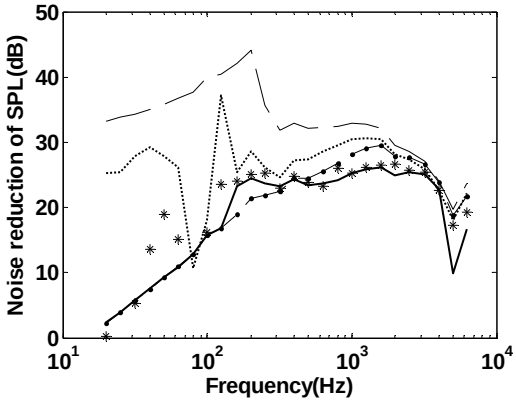

Figure 9. Difference of sound pressure level (ref: $2\times10^{-5}Pa$). (——: prediction by this study considering non-resonant response; –·–: prediction by this study ignoring non-resonant response; …..: prediction by Ming et al.'s model [2]; — —: prediction by Renji et al.'s model [8]; * : experimental results)

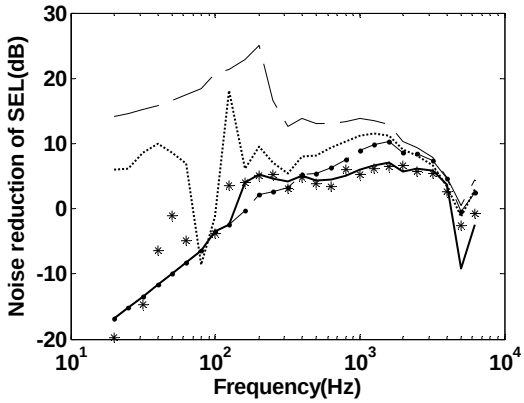

Figure 10. Difference of sound energy level (ref: $1\times10^{-12}J$). (——: prediction by this study considering non-resonant response; –·–: prediction by this study ignoring non-resonant response; …..: prediction by Ming et al.'s model [2]; — —: prediction by Renji et al.'s model [8]; * : experimental results)

Rather than using Davy's formula for the forced radiation efficiency, we have used unity forced radiation efficiency below the first non-Helmholtz natural frequency of the box. In this intermediate frequency range, the sound field in the box is controlled by Helmholtz mode which drives the volume displacement modes of the panels most effectively. The forced radiation efficiencies of those modes are at least larger than one [16]. It seems that Davy's modified formula for forced radiation efficiency is useful for NR calculation for the frequency ranges where both structure and sound field have modes. In the intermediate frequency range, the unity radiation efficiency appears to provide more accurate result. Figure 11 is the comparison results with experimental data by using the revised NR model with Davy's formula for forced radiation efficiency in the entire frequency range and the same NR model with Davy's formula [9] above the intermediate frequency range and unity radiation efficiency below the frequency. The discrepancy between Davy's prediction and experimental result is also observable in Fig.1 of [9] at intermediate frequencies.

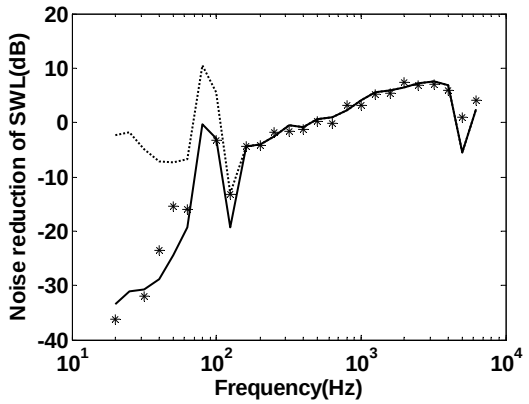

Figure 11. Difference of sound power level by using different foeced radiation efficiency (ref: $1\times10^{-12}W$). (——: prediction by this study; ……: prediction by Davy's formula [9]; * : experimental results)

CONCLUSIONS

This paper presents a more accurate SEA model for NR prediction of an acoustic enclosure at intermediate and high frequencies. The proposed model includes the non-resonant response in entire energy transfer path between the box structure and internal/external sound fields. More accurate transmission coefficient, which includes both bending stiffness and inertia in the forced radiation efficiency, is used for the coupling between the sound field and finite panels below the critical frequency. Both free and forced radiation efficiencies are important to the accuracy. The paper also provides a critical review of the previous work on NR model by Lyon, Ming and Pan, and Renji et al.. The role of non-resonance coupling is discussed in detail by discussing the discrepancies and mechanisims involved between each previous model and the experimental result. Finally, we presented the reason for using the sound power levels for the predicted and measured NR in order to avoid the possible error from the reverberation time measurement. Our future work will focus on improving the accuracy of NR in the low frequency range, and effect of heavy fluid loading on the NR modelling.

ACKNOWLEDGMENTS

This work has been undertaken in the Centre of Acoustics, Dynamics and Vibration (CADV) in the University of Western Australia, under the joined PhD program between the Northwestern Polytechanical Universtiy. The financial supports from the joined program and from CADV are gratefully acknowledged.

REFERENCES

[1] R. H. Lyon, "Noise reduction of rectangular enclosures with one flexible wall," J. Acoustic. Soc. Am. 35(11), 1791-1797 (1963)

[2] R. Ming and J. Pan, "Insertion loss of an acoustic enclosure," J. Acoustic. Soc. Am. 116(6), 3453-3459 (2004)

[3] S. M. Kim and Y. H. Kim, "Structural-acoustic coupling in a partially opened plate-cavity system: Experimental observation by using near field acoustic holography," J. Acoustic. Soc. Am. 109(1), 65-74 (2001)

[4] T. A. Osman, "Design charts for the selection of acoustical enclosures for diesel engine generator sets," J. Power and Energy, 217, 329-336 (2003)

[5] M. J. Crocker and A. J. Price, "Sound transmission using statistical energy analysis," J. Sound Vib. 9(3), 469-486 (1969)

[6] E. C. Sewell, "Transmission of reverberant sound through a single-leaf partition surround by an infinite rigid baffle," J. Sound Vib. 12(1), 21-32 (1970)

[7] D. D. Reynolds, *Engineering principles of acoustics : noise and vibration control* (MA:Ayyyn&Bacon, Boston, 1981)

[8] K. Renji, P. S. Nair and S. Narayanan, "Non-resonant response using statistical energy analysis", J. Sound Vib. 241(2), 253-270 (2001)

[9] J. L. Davy, "Predicting the sound insulation of single leaf walls: Extension of Cremer's model," J. Acoustic. Soc. Am. 126(4), 1871-1877 (2009)

[10] Y. Lei, M. P. Sheng and H. Y. Xiao, "An Improved Formula for Calculating Radiation Efficiency of Plate Around the Cut-off Frequency", J. Acta Armamentar, 30(7), 925-929 (2009)

[11] G. Xie, D. J. Thompson and C. J. C. C. Jones, "The radiation efficiency of baffled plates and strips", J. Sound Vib. 280(1), 181-209 (2005)

[12] L. Maxit, "Extension of SEA model to subsystems with non-uniform modal energy distribution," J. Sound Vib. 265(2), 337-358 (2003)

[13] V. Cotoni, P. Shorter and R. Langley, "Numerical and experimental validation of a hybrid finite element-statistical energy analysis method," J. Acoustic. Soc. Am. 122(1), 259-270 (2007)

[14] D. Jue, "Calculation of area mobility of a finite plate," Mechanical Science and Technology, 23(3), 309-311 (2004)

[15] A. J. Pretlove, "Forced vibrations of a rectangular panel backed by a closed rectangular cavity", J. Sound Vib. 3(3), 252-261 (1966)

[16] C. E. Wallace, "Radiation resistance of a rectangular panel", J. Acoustic. Soc. Am. 51, 946-952 (1972)